The Astrophysical Journal Letters, 854:L14 (8pp), 2018 February 10 https://doi.org/10.3847/2041-8213/aaaa1a

SN 2017dio: A Type-Ic Supernova Exploding in a Hydrogen-rich Circumstellar Medium*

Hanindyo Kuncarayakti[1,2], Keiichi Maeda[3,4], Christopher J. Ashall[5,6], Simon J. Prentice[5], Seppo Mattila[2], Erkki Kankare[7], Claes Fransson[8], Peter Lundqvist[8], Andrea Pastorello[9], Giorgos Leloudas[10], Joseph P. Anderson[11], Stefano Benetti[9], Melina C. Bersten[4,12,13], Enrico Cappellaro[9], Régis Cartier[14], Larry Denneau[15], Massimo Della Valle[16,17], Nancy Elias-Rosa[9], Gastón Folatelli[4,12,13], Morgan Fraser[18,35], Lluís Galbany[19], Christa Gall[10,20], Avishay Gal-Yam[21], Claudia P. Gutiérrez[22], Aleksandra Hamanowicz[23,24], Ari Heinze[15], Cosimo Inserra[7,25], Tuomas Kangas[26], Paolo Mazzali[5,27], Andrea Melandri[28], Giuliano Pignata[29,30], Armin Rest[26,31], Thomas Reynolds[2], Rupak Roy[8,32], Stephen J. Smartt[7], Ken W. Smith[7], Jesper Sollerman[8], Auni Somero[2,33], Brian Stalder[34], Maximilian Stritzinger[20], Francesco Taddia[8], Lina Tomasella[9], John Tonry[15], Henry Weiland[15], and David R. Young[7]

[1] Finnish Centre for Astronomy with ESO (FINCA), University of Turku, Väisäläntie 20, FI-21500 Piikkiö, Finland; hanindyo.kuncarayakti@utu.fi
[2] Tuorla Observatory, Department of Physics and Astronomy, University of Turku, Väisäläntie 20, FI-21500 Piikkiö, Finland
[3] Department of Astronomy, Graduate School of Science, Kyoto University, Sakyo-ku, Kyoto 606-8502, Japan
[4] Kavli Institute for the Physics and Mathematics of the Universe (WPI), The University of Tokyo, 5-1-5 Kashiwanoha, Kashiwa, Chiba 277-8583, Japan
[5] Astrophysics Research Institute, Liverpool John Moores University, IC2, Liverpool Science Park, 146 Brownlow Hill, Liverpool L3 5RF, UK
[6] Department of Physics, Florida State University, Tallahassee, FL 32306, USA
[7] Astrophysics Research Centre, School of Mathematics and Physics, Queen's University Belfast, Belfast BT7 1NN, UK
[8] The Oskar Klein Centre, Department of Astronomy, Stockholm University, AlbaNova, SE-10691 Stockholm, Sweden
[9] INAF-Osservatorio Astronomico di Padova, Vicolo dell'Osservatorio 5, I-35122 Padova, Italy
[10] Dark Cosmology Centre, Niels Bohr Institute, University of Copenhagen, Juliane Maries vej 30, DK-2100 Copenhagen, Denmark
[11] European Southern Observatory, Alonso de Córdova 3107, Vitacura, Casilla 19001, Santiago, Chile
[12] Facultad de Ciencias Astronómicas y Geofísicas, Universidad Nacional de La Plata, Paseo del Bosque S/N, B1900FWA La Plata, Argentina
[13] Instituto de Astrofísica de La Plata (IALP), CONICET, Argentina
[14] Cerro Tololo Inter-American Observatory, National Optical Astronomy Observatory, Casilla 603, La Serena, Chile
[15] Institute for Astronomy, University of Hawaii, 2680 Woodlawn Drive, Honolulu, HI 96822, USA
[16] INAF-Napoli, Osservatorio Astronomico di Capodimonte, Salita Moiariello 16, I-80131 Napoli, Italy
[17] International Center for Relativistic Astrophysics, Piazzale della Repubblica 2, I-65122, Pescara, Italy
[18] School of Physics, OBrien Centre for Science North, University College Dublin, Belfield, Dublin 4, Ireland
[19] PITT PACC, Department of Physics and Astronomy, University of Pittsburgh, Pittsburgh, PA 15260, USA
[20] Department of Physics and Astronomy, Aarhus University, Ny Munkegade 120, DK-8000 Aarhus C, Denmark
[21] Benoziyo Center for Astrophysics, Weizmann Institute of Science, 76100 Rehovot, Israel
[22] Department of Physics and Astronomy, University of Southampton, Southampton, SO17 1BJ, UK
[23] European Southern Observatory, Karl-Schwarzschild Str. 2, D-85748 Garching bei Munchen, Germany
[24] Warsaw University Astronomical Observatory, Al. Ujazdowskie 4, 00-478 Warszawa, Poland
[25] Department of Physics & Astronomy, University of Southampton, Southampton, Hampshire, SO17 1BJ, UK
[26] Space Telescope Science Institute, 3700 San Martin Drive, Baltimore, MD 21218, USA
[27] Max-Planck-Institut für Astrophysik, Karl-Schwarzschild-Str. 1, D-85748 Garching, Germany
[28] INAF—Osservatorio Astronomico di Brera, via E. Bianchi 46, I-23807, Merate (LC), Italy
[29] Departamento de Ciencias Fisicas, Universidad Andres Bello, Avda. Republica 252, Sazié, 2320, Santiago, Chile
[30] Nuncio Monseñor Sótero Sanz 100, Providencia, Santiago, Chile
[31] Department of Physics and Astronomy, The Johns Hopkins University, 3400 North Charles Street, Baltimore, MD 21218, USA
[32] Inter-University Centre for Astronomy and Astrophysics (IUCAA), Pune - 411007, India
[33] Institut de Fsica d'Altes Energies (IFAE). Edifici Cn, Universitat Autònoma de Barcelona (UAB), E-08193 Bellaterra (Barcelona), Spain
[34] LSST, 950 N. Cherry Avenue, Tucson, AZ 85719, USA

Received 2017 October 13; revised 2018 January 18; accepted 2018 January 22; published 2018 February 9

Abstract

SN 2017dio shows both spectral characteristics of a type-Ic supernova (SN) and signs of a hydrogen-rich circumstellar medium (CSM). Prominent, narrow emission lines of H and He are superposed on the continuum. Subsequent evolution revealed that the SN ejecta are interacting with the CSM. The initial SN Ic identification was confirmed by removing the CSM interaction component from the spectrum and comparing with known SNe Ic and, reversely, adding a CSM interaction component to the spectra of known SNe Ic and comparing them to SN 2017dio. Excellent agreement was obtained with both procedures, reinforcing the SN Ic classification. The light curve constrains the pre-interaction SN Ic peak absolute magnitude to be around $M_g = -17.6$ mag. No evidence of significant extinction is found, ruling out a brighter luminosity required by an SN Ia classification.

* Based on observations made with the NOT, operated by the Nordic Optical Telescope Scientific Association at the Observatorio del Roque de los Muchachos, La Palma, Spain, of the Instituto de Astrofisica de Canarias. This work is based (in part) on observations collected at the European Organisation for Astronomical Research in the Southern Hemisphere, Chile as part of PESSTO, (the Public ESO Spectroscopic Survey for Transient Objects Survey) ESO program 188.D-3003, 191.D-0935, 197.D-1075. Based on observations made with the Liverpool Telescope operated on the island of La Palma by Liverpool John Moores University in the Spanish Observatorio del Roque de los Muchachos of the Instituto de Astrofisica de Canarias with financial support from the UK Science and Technology Facilities Council.

[35] Royal Society—Science Foundation Ireland University Research Fellow.

These pieces of evidence support the view that SN 2017dio is an SN Ic, and therefore the first firm case of an SN Ic with signatures of hydrogen-rich CSM in the early spectrum. The CSM is unlikely to have been shaped by steady-state stellar winds. The mass loss of the progenitor star must have been intense, $\dot{M} \sim 0.02(\epsilon_{\mathrm{H}\alpha}/0.01)^{-1}$ $(v_{\mathrm{wind}}/500\ \mathrm{km\ s^{-1}})$ $(v_{\mathrm{shock}}/10{,}000\ \mathrm{km\ s^{-1}})^{-3}\ M_{\odot}\ \mathrm{yr^{-1}}$, peaking at a few decades before the SN. Such a high mass-loss rate might have been experienced by the progenitor through eruptions or binary stripping.

Key words: supernovae: general – supernovae: individual (SN 2017dio)

1. Introduction

Core-collapse supernovae (SNe) mark the endpoints of the evolution of massive stars. Due to mass loss, either via winds (Vink et al. 2001) or close binary interaction (Podsiadlowski et al. 1992), some of these stars end up with only a small amount of envelope left. They are thought to be the progenitors of stripped-envelope (SE) SNe, including type-Ic, Ib, and IIb SNe (Gal-Yam 2016). SNe Ic are considered to be the most highly stripped as they lack both H and He lines in their spectrum (e.g., Prentice & Mazzali 2017). Therefore, their progenitors must have experienced significant mass loss before the time of the explosion.

SNe IIn (Schlegel 1990) and Ibn (Pastorello et al. 2007) show narrow emission lines of H and He, respectively, and are thought to be interacting with a dense circumstellar medium (CSM) created through intensive mass loss of the progenitor. On the other hand, most SNe Ib/c do not show clear signs of CSM. Some examples of SNe Ib/c with signs of CSM include SNe 2014C (Milisavljevic et al. 2015), 2010mb (Ben-Ami et al. 2014), and 2001em (Chugai & Chevalier 2006). Late-time Hα emission has been detected in several luminous (Roy et al. 2016) and superluminous SNe Ic (Yan et al. 2017), and in a few SNe Ib/Ic (Vinko et al. 2017). However, H emission lines have never been observed in the early phases of SNe Ic.

SN 2017dio was discovered on 2017 April 26[36] by ATLAS[37] at 18.29 mag (cyan band). The last non-detection by ATLAS was on 2017 March 29, >19.76 mag (cyan). Subsequent spectroscopy by ePESSTO[38] on 2017 April 29 suggests that the spectrum of SN 2017dio resembles those of SNe Ic (Cartier et al. 2017). The classification spectrum also shows narrow Balmer emission lines superposed on the SN Ic spectrum. These lines yield a redshift of $z = 0.037$ that corresponds to a distance modulus of 36.0 mag, assuming $H_0 = 72\ \mathrm{km\ s^{-1}\ Mpc^{-1}}$. Line-of-sight Milky Way extinction is $E(B-V) = 0.028$ mag (Schlafly & Finkbeiner 2011). Following discovery and classification, we triggered further photometric and spectroscopic observations within the ePESSTO and NUTS[39] collaborations.

2. Observations and Data Reduction

2.1. Photometry

Optical photometry was obtained in *ugriz* filters using ALFOSC[40] at the Nordic Optical Telescope (NOT), IO:O at the Liverpool Telescope (LT), and Spectral at the 2 m telescopes of Las Cumbres Observatory. *JHK* photometry was obtained using NOT/NOTCam at one epoch, 2017 July 27.

Standard reduction techniques were applied using IRAF,[41] and aperture photometry was carried out for the SN and surrounding stars. Photometric zero points were derived by comparing the instrumental magnitudes of the stars in the field to photometry from Sloan Digital Sky Survey, Data Release 14.[42] Additionally, pre-discovery *V*-band data points were obtained from the CRTS[43] archive and these were scaled to have the data point at 2017 May 01 match the *g*-band data point at the same epoch.

2.2. Spectroscopy

Optical slit-spectroscopy was obtained using ALFOSC at the NOT, EFOSC2[44] at the ESO New Technology Telescope (NTT, through the ePESSTO program), and SPRAT[45] at the LT. ALFOSC spectra cover 3300–9500 Å, with a resolution of 16 Å. With EFOSC2, grism #13, the coverage was 3500–9300 Å, at a 21 Å resolution. Additionally, in two epochs the EFOSC2 spectra were taken using grism #11 (16 Å resolution). SPRAT covers 4000–8000 Å, with a 18 Å resolution.

After the standard reduction procedures, the spectra were extracted, then wavelength and flux calibrated. IRAF, FOSCGUI,[46] and PESSTO pipeline[47] tools were used in the procedures.

3. Results and Discussion

3.1. Spectra and Evolution

At four days post-discovery, SN 2017dio was classified as an SN Ic. The subsequent spectra at +5 and +6 days (+0 days being the discovery date) are very similar in appearance to the classification spectrum (Figure 1). The spectra are relatively smooth, with broad features at wavelength ranges ~4000–5500 and ~8000–9000 Å. There are emission lines of H and He I at $\lambda\lambda$5876, 7065. At +18 days, the continuum becomes almost featureless and after this point the spectrum starts to show evolving features. Both H and He emission lines are always present, and are resolved by our instruments, with Lorentzian full-width at half-maximum (FWHM) corresponding to an expansion velocity of ~500 km s^{-1} (corrected for instrumental broadening). These lines are therefore not originating from an underlying H II region and are more likely attributed to the SN CSM.

The early light curve (LC) of SN 2017dio was found to be rising (Figure 2). While the presence of narrow H emission features would put SN 2017dio into the SN IIn subclass, the underlying continuum does not show the typical blue featureless early spectrum (see, e.g., Kiewe et al. 2012; Taddia et al. 2013). At later phases, it became strikingly similar to some SNe IIn (Figure 1). The original SN Ic classification was

[36] Dates are UTC throughout the Letter.
[37] The Asteroid Terrestrial-impact Last Alert System (Tonry 2011).
[38] Extended Public ESO Spectroscopic Survey of Transient Objects (Smartt et al. 2015).
[39] Nordic Optical Telescope Unbiased Transient Survey (Mattila et al. 2016).
[40] Andalucia Faint Object Spectrograph and Camera.
[41] http://iraf.net/
[42] http://www.sdss.org/dr14/
[43] Catalina Real-Time Transient Survey (Drake et al. 2009).
[44] ESO Faint Object Spectrograph and Camera 2 (Buzzoni et al. 1984).
[45] Spectrograph for the Rapid Acquisition of Transients (Piascik et al. 2014).
[46] http://sngroup.oapd.inaf.it/foscgui.html
[47] https://github.com/svalenti/pessto

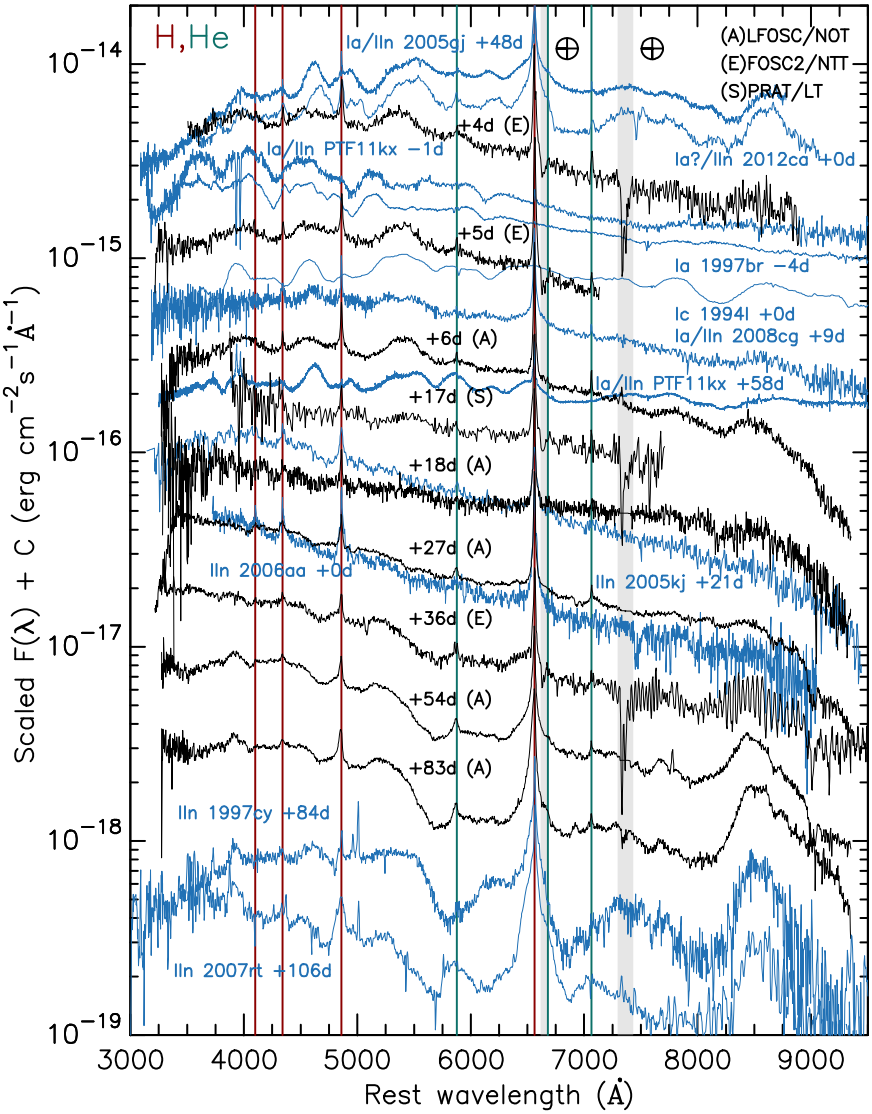

Figure 1. Spectral sequence of SN 2017dio. Comparison spectra of other SNe (obtained through WISeREP—https://wiserep.weizmann.ac.il/—Yaron & Gal-Yam 2012) are plotted in blue. Phases for SN 2017dio are days after the discovery, while for other SNe phases are post maximum. The rest wavelengths of the H I lines are indicated with dark red and He I with dark green lines. Telluric absorption regions in SN 2017dio spectra are indicated with gray shading. SN 2017dio spectra will be made publicly available at WISeREP and the Open Supernova Catalog (https://sne.space/; Guillochon et al. 2017).

obtained by omitting these emission lines and only inspecting the underlying spectrum. In the case of SNe IIn, the narrow emission lines are considered to be a sign of CSM, whereas the underlying SN in SNe IIn is hidden. SN 2017dio becomes quite clearly an SN IIn after +18 days, but at early phases shows broad absorption/emission features typical of an SE SN. As such, it provides a rare opportunity to investigate the underlying SN type in SNe IIn.

A number of objects in the literature have been considered to be either SN Ia or Ic, such as SNe 2002ic (Hamuy et al. 2003; Benetti et al. 2006) and 2012ca (Fox et al. 2015; Inserra et al. 2016), due to the spectral similarities of SNe Ia and Ic particularly in the early phase. Nevertheless, the majority of these objects are believed to be SNe Ia embedded in a dense CSM (Silverman et al. 2013; Leloudas et al. 2015). PTF11kx (Dilday et al. 2012) is considered to be a clear example of a bona fide SN Ia with CSM interaction, as the SN was relatively interaction-free in the early phase. In Figure 1, it can be seen that there are similarities between SN 2017dio at the early phase with both SNe Ia and Ic; however, no exact match was found and its spectral appearance cannot be reproduced by any of those interacting SNe Ia.

One way to reassess the classification is by removing the spectral component attributed to the CSM interaction, and then cross-matching the spectrum with a template of SNe with various types. For this purpose, the +18 day spectrum was used as a proxy for the CSM interaction spectrum, and subtracted from the +6 day spectrum to obtain a "pure" SN component. Before subtraction, the spectra were normalized by the average flux across the wavelength range. The first spectrum in Figure 3 (left) shows the subtraction result, compared to several other SNe. The SNID (Blondin & Tonry 2007) and GELATO (Harutyunyan et al. 2008) tools were used to compare this spectrum with those of known SNe. Both tools yield an SN Ic classification around the maximum light, and a better match is obtained with broad-lined SN Ic (hereafter SN IcBL) spectra than with normal SN Ic. However, a precise classification is difficult at these epochs (Prentice & Mazzali 2017). Other SN types (Ia, Ib, II) do not provide a better match compared to SN Ic.

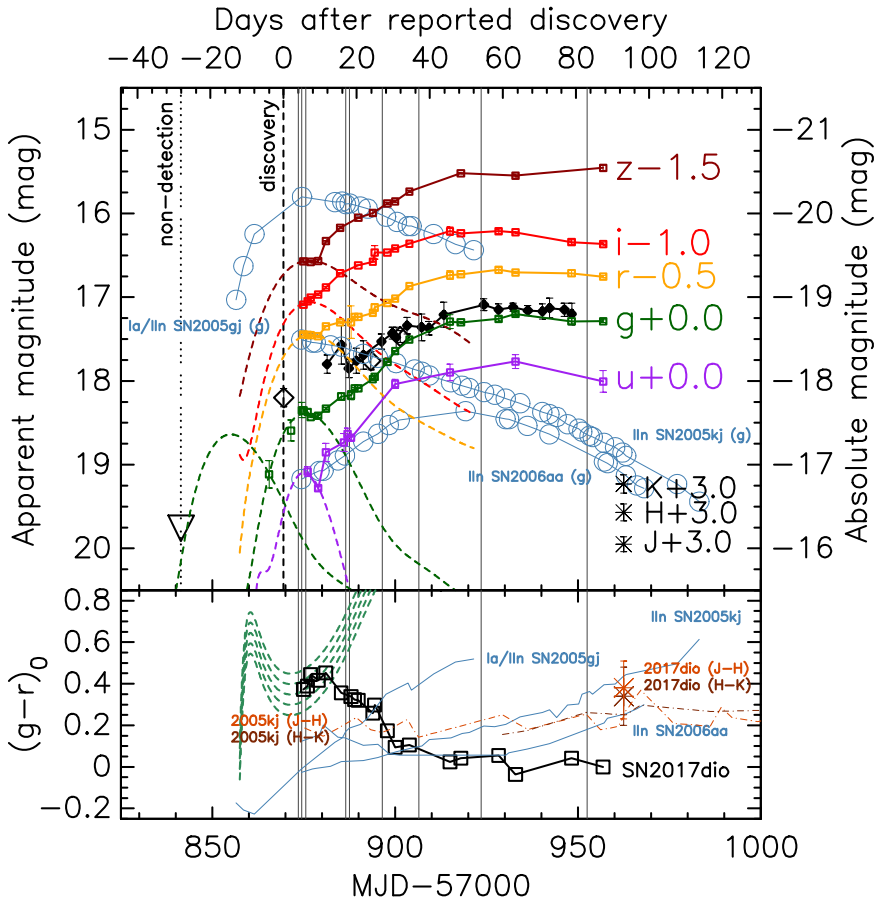

Figure 2. (Top) Light curves of SN 2017dio in *ugriz* bands, and *JHK* photometric points. CRTS data points are plotted as *g*-band but not connected to the *g*-band LC. The absolute magnitudes assume only the distance modulus of 36.0 mag. ATLAS cyan band (open black diamonds) and orange band (filled black diamonds) data points are plotted. A non-detection (3σ) limiting magnitude is plotted with an upside-down triangle. Vertical gray lines indicate the epochs of spectroscopy. Dashed curves represent template SNe Ic LCs of Taddia et al. (2015). Another solution for the *g*-band LC peaking before the discovery is also plotted. The LCs of SNe 2005gj (Aldering et al. 2006; Holtzman et al. 2008), 2005kj and 2006aa (Taddia et al. 2013) in *g*-band absolute magnitude are shown in blue, with their phases shifted to have the peak (SN 2005gj) or discovery epoch (SNe 2005kj, 2006aa) matching the SN Ic LC peak. (Bottom) Color curves of SNe 2017dio, 2005gj, 2005kj, and 2006aa, in $(g-r)_0$ (corrected for foreground extinction). The green dashed area represents typical SNe Ic (Taddia et al. 2015). $(J-H)$ and $(H-K)$ colors are plotted in comparison to SN 2005kj.

To check the validity of this method, a reverse procedure was applied: the +18 day spectrum representing CSM interaction was coadded to templates of known SN spectra. Leloudas et al. (2015) simulated various pure SN spectra coadded to a CSM interaction component to investigate the spectral identification of SNe IIn, and showed that the flux ratio of the underlying SN to the continuum f_V is the most important parameter determining if an underlying, intrinsic SN spectrum can be classified correctly. Following Leloudas et al. (2015), we experimented with varying f_V to match the appearance of the coadded spectra with the +6 day spectrum. We found that the +6 day SN 2017dio spectrum is best matched by type-Ic SNe coadded to the CSM interaction spectrum with $f_V \gtrsim 0.3$ (Figure 3, right). This is consistent with the finding of Leloudas et al. (2015) that a critical $f_V \gtrsim 0.3$ is needed in order to correctly classify an underlying pure SN Ic spectrum contaminated by CSM interaction. Below $f_V \approx 0.3$, these events would be indistinguishable from typical SN IIn without a hint of the nature of the underlying SN.

These analyses suggest that SN 2017dio underwent a transition from type Ic to IIn. The SN Ic spectrum was prominent in the early phases, while at later times the CSM interaction component dominates. A signature of the increasing strength of CSM interaction is the broadening of the emission lines. Figure 4 shows the evolution of the strongest H and He lines, showing their widths increasing with time. The Lorentzian FWHM of the lines was typically around 500 km s^{-1} at the beginning and increased to ∼2000 km s^{-1} in the later spectra. The line profile was initially symmetric with wings indicative of electron scattering (e.g., Dessart et al. 2016), then evolved into an asymmetric profile with a broad blue component. This evolution is similar to that seen in SN 2010jl, where such an asymmetric profile may be caused by dust (Gall et al. 2014), or alternatively radiative acceleration or radiative transfer effects in the cool dense shell (Fransson et al. 2014). Nevertheless, in the early phase of SN 2017dio, such a profile is not observed. The observed optical color evolution showing SN 2017dio becoming bluer with time and the Hα/Hβ line ratio staying relatively constant in these epochs do not support dust formation (Figures 2 and 5). Furthermore, the observed near-infrared colors are consistent with those expected for an SN IIn without any significant excess emission from dust (Taddia et al. 2013). Therefore, we do not expect dust to affect our observations.

As the spectral evolution points to SN 2017dio being an SN Ic interacting with CSM, the LC should also match this interpretation. The underlying SN Ic luminosity must be fainter compared to the observed LC that includes the CSM interaction

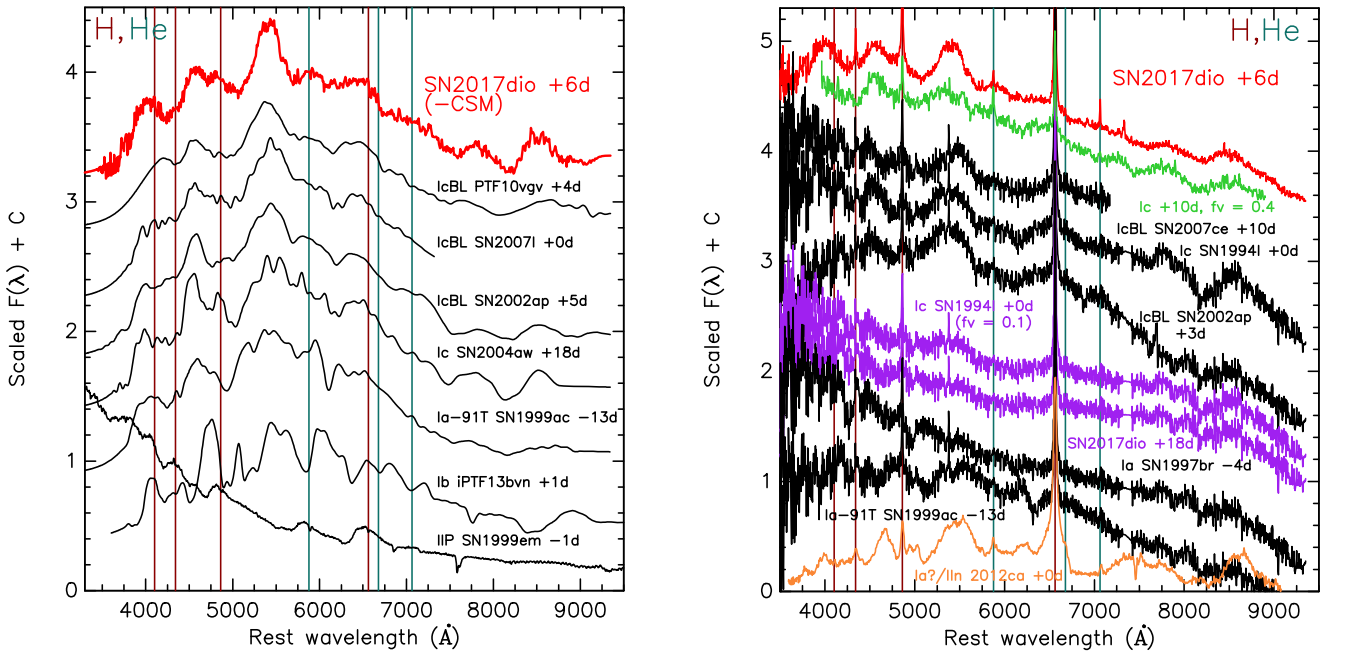

Figure 3. (Left) Comparison of the CSM interaction-subtracted spectrum of SN 2017dio (red) with spectra of other SNe (black; including SNID templates of Modjaz et al. 2014). (Right) Comparison of the +6 day spectrum of SN 2017dio (red) with those of other SNe combined with interaction spectrum (black; $f_V = 0.3$), a template SN Ic+CSM interaction spectrum from Leloudas et al. (2015, green), and SN 2012ca (orange). The spectrum of SN 1994I combined with the interaction spectrum ($f_V = 0.1$) is showed for comparison with SN 2017dio at +18 days. The comparison spectra are from WISeREP. In both panels, phases are days from maximum for spectra other than SN 2017dio.

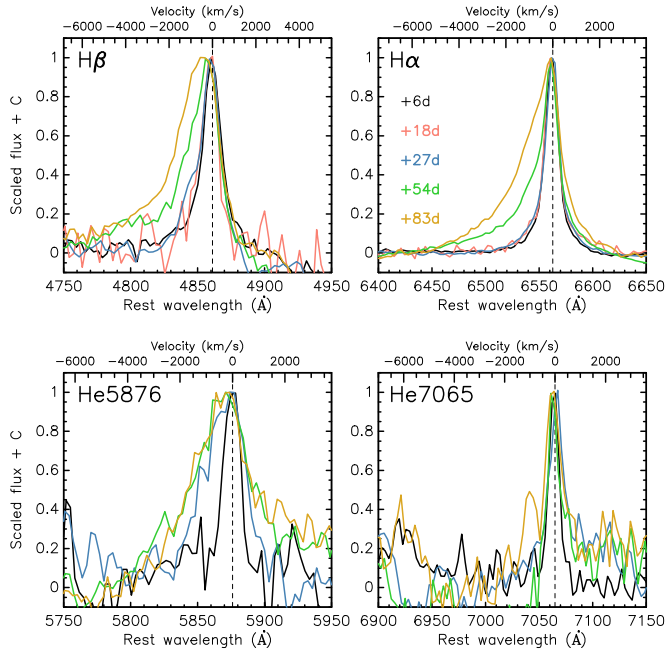

Figure 4. Observed line profile evolution for Hα, Hβ, He I λ5876, and He I λ7065. Only data taken with the same instrument and setting (ALFOSC) are plotted, for clarity.

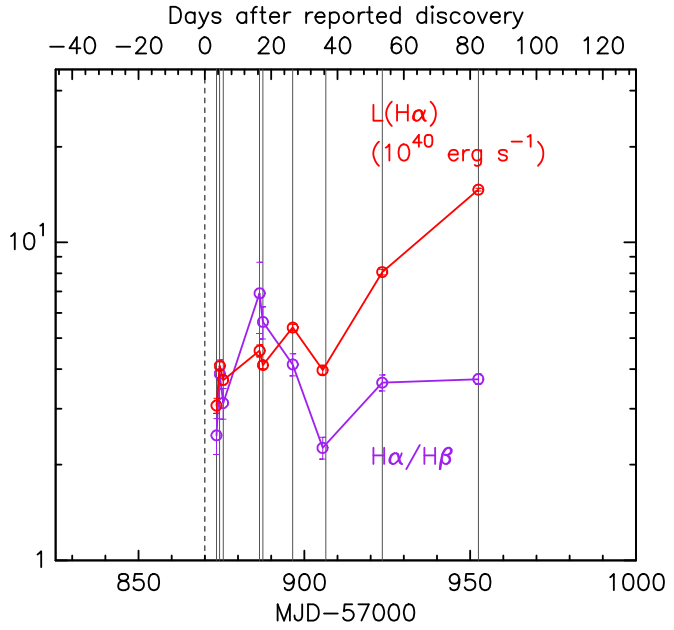

Figure 5. Evolution of the Hα/Hβ flux ratio (purple), and Hα line luminosity (red).

contribution. In Figure 2, we plot template SN Ic LCs from Taddia et al. (2015) to match our photometry. The epochs of the template LCs are the same, and they are only shifted vertically. It is apparent that the template LC peak corresponds to the epoch of the first spectra. This is consistent with the spectral match to SNe Ic around the peak. In a few days, the observed LC continued rising and there was a flux offset between the observed and template LCs. Since then, the subsequent photometric evolution can be explained by the increasing contribution from the interaction. The Hα line luminosity is generally increasing, suggesting an increasing strength of the interaction (Figure 5). Interaction appears to have started about the time of the SN Ic LC peak, yielding extra flux in the observed LC at subsequent phases, and eventually broadening the emission lines.

The observed LC of SN 2017dio peaked at around early 2017 July (MJD $\sim$ 57930), about 60 days after the discovery and during the interaction dominated phase. The peak absolute

magnitude was $M_g = M_r = -18.8$ mag. Leloudas et al. (2015) estimated the peak luminosity needed for CSM interaction to hide an SN Ic/IcBL. A SN IIn needs to reach at least approximately −19 mag to hide an SN Ic peaking at approximately −17.5 mag. In Figure 2, the underlying photospheric SN Ic LC might have reached $M_g = -17.6$ mag at peak, which is consistent with the above scenario. A second solution to the LC peak can be placed between the last non-detection and the first photometric point (Figure 2); nevertheless, this would yield a similar, perhaps even fainter, peak magnitude. The corresponding photospheric peak magnitude of $M_r = -18.1$ mag is well within the observed distributions of SNe Ic and IcBL ($M_R = -18.5 \pm 0.8$ mag and $M_R = -19.0 \pm 1.1$ mag, respectively; Drout et al. 2011). SNe Ia with CSM interaction are found to peak brighter than $M_V \sim -19.5$ mag (Silverman et al. 2013; Leloudas et al. 2015), which is constrained by the underlying SN Ia LC peaking between −18.5 and −19.7 mag. These luminosity ranges cannot accommodate both the observed LC peak and the underlying SN Ic photospheric LC peak in SN 2017dio. In SNe Ia with CSM interaction, the underlying SN is always spectroscopically similar to the SN 1991T-like objects, which is a brighter subgroup of SNe Ia. They are spectroscopically distinguishable from SN Ic (e.g., Leloudas et al. 2015) and the spectra of SN 2017dio do not show similarities with these objects. The extinction toward SN 2017dio appears to be negligible (i.e., no sign of Na I absorption or high Balmer decrement, and normal colors), ruling out a higher intrinsic luminosity that would be required by the scenario for an SN Ia with CSM interaction.

The consistency between the spectral and photometric evolutions suggests that the interpretation of SN 2017dio being an SN Ic interacting with a CSM and transitioning into an SN IIn is robust. Alternative explanations such as SN Ia, II, or Ib with CSM interaction are not plausible.

3.2. Host Galaxy

The field of SN 2017dio is in the SDSS database. The host galaxy, SDSS J113627.76+181747.3, has $u = 23.36$, $g = 21.12$, $r = 20.67$, $i = 20.55$, and $z = 20.12$ mag. Considering the distance modulus and foreground reddening, the absolute magnitude is $M_g = -15.1$ mag. The galaxy appears to be small without a discernible shape. Its diameter of $\sim 3''$ corresponds to ∼2 kpc at the distance of ∼160 Mpc. This suggests that the host is a dwarf galaxy smaller and fainter than the Small Magellanic Cloud ($M_V = -16.8$ mag, McConnachie 2012).

In the spectra of SN 2017dio, the interstellar emission lines from the galaxy are hidden by the SN. Therefore, no strong-line analyses such as estimates of star formation rate or metallicity can be done. Employing the galaxy luminosity–metallicity relation of Tremonti et al. (2004) yields an estimate of $12 + \log(\mathrm{O/H}) \approx 8.0$ dex for the galaxy. Comparing this luminosity to the sample of SN Ic and IcBL hosts (Modjaz et al. 2008), the host of SN 2017dio falls at the faint end of the distribution. Dwarf galaxies with the size of SN 2017dio host predominantly produce SNe IcBL rather than normal SNe Ic (Arcavi et al. 2010). This is also consistent with the possibility that SN 2017dio is an SN IcBL.

3.3. CSM and Progenitor Characteristics

The spectra and LC show that the CSM interaction was relatively weak at the earliest epochs. Therefore, the bulk of the CSM is not located at the immediate vicinity of the progenitor star. The SN ejecta must have traveled outward in a rarefied environment before encountering the denser CSM parts. The Hα/Hβ line ratio was around 3 in the early phases and two times higher after two weeks, consistent with increasing CSM densities. After this peak, the Hα/Hβ ratio drops and rises again, indicating fluctuations in the CSM density (Figure 5). In a $\rho \sim r^{-2}$ spherically distributed CSM created by steady-state stellar winds (Chevalier & Fransson 1994), such behavior is not expected.

At the early epochs, the emission lines are narrow with symmetric wings. They are likely to arise from continuous ionization by the interaction of the shock with the CSM, and effects of electron scattering within the CSM. The later spectra show asymmetric lines with broad blue wings (Figure 4). The asymmetric line profile may be caused by the interaction region being occulted at the receding side of the optically thick ejecta, thus causing the red wing to be suppressed. At the earliest epochs, the CSM interaction was weak, and thus the SN Ic spectral characteristics were visible. Later, when the CSM interaction dominates, the SN Ic features are hidden by the CSM interaction component.

Thus, the geometry of the CSM embedding SN 2017dio progenitor does not seem to be consistent with that generated from spherically symmetric mass loss via winds. Instead, it could have a clumpy, toroidal, or even bipolar distribution. With the averaged expansion velocity of 10,000 km s^{-1} for SNe Ib/c (e.g., Cano 2013), the SN ejecta took 80 days to reach the part of the CSM corresponding to the peak Hα luminosity. This translates into a distance of ∼500 au. Presumably, this part of the CSM was created through mass loss with a velocity of 500 km s^{-1}. The luminosity of the Hα line can be used to estimate the mass-loss rate of the progenitor star responsible for the CSM build-up in the vicinity, as Hα luminosity is proportional to the kinetic energy dissipated per unit time. The observed peak Hα luminosity of SN 2017dio is $\sim 1.5 \times 10^{41}$ erg s^{-1}. The peak Hα luminosity can be used to estimate the progenitor mass-loss rate by employing the relation

$$\dot{M} = 2 \frac{L_{\mathrm{H}\alpha}}{\epsilon_{\mathrm{H}\alpha}} \frac{v_{\mathrm{wind}}}{(v_{\mathrm{shock}})^3}. \quad (1)$$

Assuming a progenitor wind velocity of 500 km s^{-1} from emission line FWHM at the early epochs, and an efficiency factor $\epsilon_{\mathrm{H}\alpha}$ of 0.01 (Chevalier & Fransson 1994), the pre-SN mass-loss rate of the progenitor star was estimated to be $\sim 0.02 (\epsilon_{\mathrm{H}\alpha}/0.01)^{-1}$ $(v_{\mathrm{wind}}/500\ \mathrm{km\ s^{-1}})$ $(v_{\mathrm{shock}}/10{,}000\ \mathrm{km\ s^{-1}})^{-3}$ $M_\odot$ yr^{-1}. The shock velocity must be lower compared to the velocity of the part of the ejecta that is not interacting with the CSM, but this is hidden by the electron scattering wings, which extend up to ∼10,000 km s^{-1} (Figure 4). The derived progenitor mass-loss rate is comparable to some SNe IIn (Kiewe et al. 2012; Taddia et al. 2013). It is a few times lower compared to SN 2010jl ($\dot{M} \sim 0.1\ M_\odot$ yr^{-1}, and consistently, so are the peak bolometric[48] and Hα luminosities (∼10^{43} erg s^{-1} and ∼10^{41} erg s^{-1}, respectively, compared to ∼3 × 10^{43} erg s^{-1} and ∼10^{42} erg s^{-1}; Fransson et al. 2014).

The progenitor must therefore have experienced major mass loss a few decades before the SN. Then, the rest of the envelope was removed through less vigorous mass loss in the final years, until being removed completely prior to the SN. This is

[48] Calculated from the g-band light curve and ($g-$r) colors using the simple prescription of Lyman et al. (2014).

reminiscent of the inferred progenitor behavior of the type-Ib/IIn SN 2014C (Milisavljevic et al. 2015). High pre-SN mass loss may be caused by eruptions (e.g., Smith & Arnett 2014) or stripping by a close binary companion (e.g., Yoon et al. 2017). With a wind-driven mass loss, it is inconceivable for the progenitor to still retain the H-rich material nearby while the He layer is depleted, as observed in SN 2017dio. In the binary progenitor scenario, the primary transfers material to the secondary through a Roche-lobe overflow and evolves into a C+O star. With an increased mass, the secondary's evolution is accelerated and it leaves the main sequence before the explosion of the primary. The secondary then experiences a luminous blue variable (LBV) phase, or becomes a giant and starts a reverse mass transfer to the primary. At this point there is a large amount of H-rich CSM around the primary and it explodes as an SN Ic. This path could have occurred within the standard binary evolution, and the progenitor system may be somewhat similar to some Wolf-Rayet+LBV binaries such as HD 5980 (Koenigsberger et al. 2014). The prototypical type Ibn SN 2006jc experienced a giant outburst two years prior to the SN (Pastorello et al. 2007). A possible lower-mass companion star detected in late-time observations together with the lack of further outbursts after the explosion suggest that the outburst originated from the SN progenitor itself (Maund et al. 2016). Given that SN 2017dio could be an SN IcBL, we note that binary evolution may also play an important role for SNe IcBL.

4. Summary

The early spectrum of SN 2017dio resembles those of SNe Ic, with a CSM component. SN 2017dio appears to be brightening after the discovery, accompanied by an increase of Hα luminosity and a broadening of the emission lines. This is consistent with CSM interaction becoming dominant. The evolution suggests that the epoch of maximum for the underlying SN Ic was around the discovery. With this constraint, the peak luminosity of SN 2017dio falls into the range commonly observed for SNe Ic.

The CSM must not have been distributed as $\rho \sim r^{-2}$, typical for a steady-state stellar wind. This would require that the progenitor star underwent vigorous mass-loss episodes a few decades before the SN, possibly driven by eruption or binary interaction.

We thank the referee and Sung-Chul Yoon for useful suggestions. K.M. acknowledges the FINCA visitor program, Japan Society for the Promotion of Science (JSPS) through KAKENHI Grant 17H02864 and JSPS Open Partnership Bilateral Joint Research Project between Japan and Chile. L.G. was supported by the US National Science Foundation, Grant AST-1311862. C.P.G. acknowledges EU/FP7-ERC grant No. [615929]. A.P., S.B., L.T., and N.E.R. are supported by the PRIN-INAF 2014 project Transient Universe: unveiling new types of stellar explosions with PESSTO. Support for G.P. is provided by the Ministry of Economy, Development, and Tourism's Millennium Science Initiative through grant IC120009, awarded to The Millennium Institute of Astrophysics, MAS. C.G. is supported by the Carlsberg Foundation. M.D.S. is supported by a research grant (13261) from the VILLUM FONDEN. NUTS is supported in part by IDA (Instrumentcenter for Danish Astrophysics). The ATLAS surveys are funded through NASA grants NNX12AR55G. A.G.-Y. is supported by the EU via ERC grant No. 725161, the Quantum Universe I-Core program, the ISF, the BSF Transformative program and by a Kimmel award.

Facilities: NOT(ALFOSC, NOTCam), NTT(EFOSC2), Liverpool:2m, LCOGT: 2m.

ORCID iDs

Hanindyo Kuncarayakti https://orcid.org/0000-0002-1132-1366
Simon J. Prentice https://orcid.org/0000-0003-0486-6242
Seppo Mattila https://orcid.org/0000-0001-7497-2994
Erkki Kankare https://orcid.org/0000-0001-8257-3512
Claes Fransson https://orcid.org/0000-0001-8532-3594
Peter Lundqvist https://orcid.org/0000-0002-3664-8082
Giorgos Leloudas https://orcid.org/0000-0002-8597-0756
Joseph P. Anderson https://orcid.org/0000-0003-0227-3451
Enrico Cappellaro https://orcid.org/0000-0001-5008-8619
Massimo Della Valle https://orcid.org/0000-0003-3142-5020
Morgan Fraser https://orcid.org/0000-0003-2191-1674
Lluís Galbany https://orcid.org/0000-0002-1296-6887
Christa Gall https://orcid.org/0000-0002-8526-3963
Avishay Gal-Yam https://orcid.org/0000-0002-3653-5598
Claudia P. Gutiérrez https://orcid.org/0000-0002-7252-4351
Cosimo Inserra https://orcid.org/0000-0002-3968-4409
Tuomas Kangas https://orcid.org/0000-0002-5477-0217
Paolo Mazzali https://orcid.org/0000-0001-6876-8284
Giuliano Pignata https://orcid.org/0000-0003-0006-0188
Rupak Roy https://orcid.org/0000-0002-9711-6207
Stephen J. Smartt https://orcid.org/0000-0002-8229-1731
Jesper Sollerman https://orcid.org/0000-0003-1546-6615
Auni Somero https://orcid.org/0000-0001-6566-9192
Maximilian Stritzinger https://orcid.org/0000-0002-5571-1833
Lina Tomasella https://orcid.org/0000-0002-3697-2616
John Tonry https://orcid.org/0000-0003-2858-9657
David R. Young https://orcid.org/0000-0002-1229-2499

References

Aldering, G., Antilogus, P., Bailey, S., et al. 2006, ApJ, 650, 510
Arcavi, I., Gal-Yam, A., Kasliwal, M. M., et al. 2010, ApJ, 721, 777
Ben-Ami, S., Gal-Yam, A., Mazzali, P. A., et al. 2014, ApJ, 785, 37
Benetti, S., Cappellaro, E., Turatto, M., et al. 2006, ApJL, 653, L129
Blondin, S., & Tonry, J. L. 2007, ApJ, 666, 1024
Buzzoni, B., Delabre, B., Dekker, H., et al. 1984, Msngr, 38, 9
Cano, Z. 2013, MNRAS, 434, 1098
Cartier, R., Gutierrez, C. P., Smith, M., et al. 2017, ATel, 10334
Chevalier, R. A., & Fransson, C. 1994, ApJ, 420, 268
Chugai, N. N., & Chevalier, R. A. 2006, ApJ, 641, 1051
Dessart, L., Hillier, D. J., Audit, E., Livne, E., & Waldman, R. 2016, MNRAS, 458, 2094
Dilday, B., Howell, D. A., Cenko, S. B., et al. 2012, Sci, 337, 942
Drake, A. J., Djorgovski, S. G., Mahabal, A., et al. 2009, ApJ, 696, 870
Drout, M. R., Soderberg, A. M., Gal-Yam, A., et al. 2011, ApJ, 741, 97
Fox, O. D., Silverman, J. M., Filippenko, A. V., et al. 2015, MNRAS, 447, 772
Fransson, C., Ergon, M., Challis, P. J., et al. 2014, ApJ, 797, 118
Gall, C., Hjorth, J., Watson, D., et al. 2014, Natur, 511, 326
Gal-Yam, A. 2016, in Handbook of Supernovae, ed. A. W. Alsabti & P. Murdin (Berlin: Springer), in press (arXiv:1611.09353)
Guillochon, J., Parrent, J., Kelley, L. Z., & Margutti, R. 2017, ApJ, 835, 64
Hamuy, M., Phillips, M. M., Suntzeff, N. B., et al. 2003, Natur, 424, 651
Harutyunyan, A. H., Pfahler, P., Pastorello, A., et al. 2008, A&A, 488, 383
Holtzman, J. A., Marriner, J., Kessler, R., et al. 2008, AJ, 136, 2306
Inserra, C., Fraser, M., Smartt, S. J., et al. 2016, MNRAS, 459, 2721
Kiewe, M., Gal-Yam, A., Arcavi, I., et al. 2012, ApJ, 744, 10
Koenigsberger, G., Morrell, N., Hillier, D. J., et al. 2014, AJ, 148, 62

Leloudas, G., Hsiao, E. Y., Johansson, J., et al. 2015, A&A, 574, A61
Lyman, J. D., Bersier, D., & James, P. A. 2014, MNRAS, 437, 3848
Mattila, S., Elias-Rosa, N., Lundqvist, P., et al. 2016, ATel, 8992
Maund, J. R., Pastorello, A., Mattila, S., Itagaki, K., & Boles, T. 2016, ApJ, 833, 128
McConnachie, A. W. 2012, AJ, 144, 4
Milisavljevic, D., Margutti, R., Kamble, A., et al. 2015, ApJ, 815, 120
Modjaz, M., Blondin, S., Kirshner, R. P., et al. 2014, AJ, 147, 99
Modjaz, M., Kewley, L., Kirshner, R. P., et al. 2008, AJ, 135, 1136
Pastorello, A., Smartt, S. J., Mattila, S., et al. 2007, Natur, 447, 829
Piascik, A. S., Steele, I. A., Bates, S. D., et al. 2014, Proc. SPIE, 9147, 91478H
Podsiadlowski, P., Joss, P. C., & Hsu, J. J. L. 1992, ApJ, 391, 246
Prentice, S. J., & Mazzali, P. A. 2017, MNRAS, 469, 2672
Roy, R., Sollerman, J., Silverman, J. M., et al. 2016, A&A, 596, A67
Schlafly, E. F., & Finkbeiner, D. P. 2011, ApJ, 737, 103
Schlegel, E. M. 1990, MNRAS, 244, 269
Silverman, J. M., Nugent, P. E., Gal-Yam, A., et al. 2013, ApJS, 207, 3
Smartt, S. J., Valenti, S., Fraser, M., et al. 2015, A&A, 579, A40
Smith, N., & Arnett, W. D. 2014, ApJ, 785, 82
Taddia, F., Sollerman, J., Leloudas, G., et al. 2015, A&A, 574, A60
Taddia, F., Stritzinger, M. D., Sollerman, J., et al. 2013, A&A, 555, A10
Tonry, J. L. 2011, PASP, 123, 58
Tremonti, C. A., Heckman, T. M., Kauffmann, G., et al. 2004, ApJ, 613, 898
Vink, J. S., de Koter, A., & Lamers, H. J. G. L. M. 2001, A&A, 369, 574
Vinko, J., Pooley, D., Silverman, J. M., et al. 2017, ApJ, 837, 62
Yan, L., Lunnan, R., Perley, D. A., et al. 2017, ApJ, 848, 6
Yaron, O., & Gal-Yam, A. 2012, PASP, 124, 668
Yoon, S.-C., Dessart, L., & Clocchiatti, A. 2017, ApJ, 840, 10